Energy spectrum and barrier localization of quantum well electrons in parallel magnetic fields

1991 J. Phys.: Condens. Matter 3 6425

(http://iopscience.iop.org/0953-8984/3/33/019)

J. Phys.: Condens. Matter 3 (1991) 6425–6432. Printed in the UK

Energy spectrum and barrier localization of quantum well electrons in parallel magnetic fields

G Marx†, B Huckestein‡ and R Kümmel†

† Physikalisches Institut der Universität Würzburg, D-8700 Würzburg, Federal Republic of Germany

‡ Physikalisch-Technische Bundesanstalt, Postfach 3345, D-3300 Braunschweig, Federal Republic of Germany

Received 22 January 1991, in final form 22 April 1991

Abstract. The magnetically tunable energy spectrum and the charge density distributions of electrons in GaAs–AlGaAs quantum wells with magnetic fields parallel to the interfaces are calculated both analytically and numerically. For states below the barrier edge and magnetic fields up to 15–20 T both methods yield nearly identical results. There are two types of localized states above the barrier. They originate from shallow depressions of the effective potential and from interferences.

1. Introduction

Recently, a new, graph-supported analytical method (arrow train method) has been developed in order to calculate the energy eigenvalues and wavefunctions of electrons in an infinitely deep quantum well (QW) with a magnetic field oriented parallel to the potential walls [1]. Subsequently, the method has been generalized for the treatment of QWs of finite depth in parallel fields, and the resulting energy spectrum was used in the computation of the magnetization which oscillates as a function of the chemical potential [2]. The purpose of the present paper is twofold: first we present the analytical calculation of this spectrum which neglects the magnetic field in the barrier and is thus strictly valid only for the low lying energy states. Second by numerically integrating the Schrödinger equation we obtain the full energy spectrum and the charge density distribution of the individual eigenstates. Thus, the deviations of the results of the analytical approximation from the ones of the exact numerical computations can be determined. Furthermore, we look for and find localized barrier states which are to be expected for appropriate 'centre of orbit' coordinates [3, 4].

2. Approximate analytical energy spectrum and wavefunctions

In this section we extend the arrow train method to isolated rectangular QWs with barriers of finite height V. We will first describe the mathematical method employed in [1] in solving the eigenvalue problem and later we will indicate the modifications to those equations in [1] which are affected by the finite barrier height.

To solve the eigenvalue problem the wavefunction in the Schrödinger equation is first expanded in a power series. Since the Hamiltonian is that of a harmonic oscillator

0953-8984/91/336425+08$03.50

in a box it contains only second-order derivatives and a second-order polynomial. Thus the Schrödinger equation in matrix notation contains non-zero elements only on a few diagonals near the main diagonal. Together with the equations arising from the boundary conditions we get an infinite set of linear equations for the expansion coefficients of the wavefunction. The eigenvalues are given by the condition that its determinant must vanish.

For this determinant a power series representation can be derived as a function of the parameters appearing in the Schrödinger equation, i.e. energy, magnetic field strength and wavevector. This representation can then be inverted to get the energy as a power series of magnetic field strength and wavevector. The coefficients of this power series expansion are given analytically. In order to derive the power series representation of the determinant it is expanded with respect to the rows arising from the boundary conditions. This gives an infinite sum over infinite minors. Due to the nature of the Hamiltonian and the power series expansion of the wavefunction these infinite minors can be factorized into a finite part and an infinite minor of value unity. The remaining minors of finite order are almost triangular. A recursion relation can be established that allows the minors to be brought to a fully triangular shape and, hence, allow the calculation of the minors. With a graph-supported arrow train method this recursion relation can be solved for an arbitrary order of the minors. This yields a power series representation of the determinant as a function of energy, magnetic field and wavevector with coefficients given by analytical expressions. Setting the determinant equal to zero and solving for the energy results in a power series in magnetic field and wavevector, again with coefficients given by analytical expressions. Once these coefficients have been calculated one can compute exactly the spectrum of any QW with infinite barrier potential at any magnetic field.

The extension of the method to QWs with finite barrier height is briefly sketched in the following. The QW extends in the z-direction from $-\frac{1}{2}$ to $\frac{1}{2}$ in coordinates normalized to the well width a. The magnetic field is $e_x B_\parallel$, and the corresponding vector potential is chosen to be $\boldsymbol{A} = -e_y z a B_\parallel$. (The orientation of the parallel field is different from the one in [1] in order to have Maan's gauge [5] in the general case of a tilted field, to be discussed in a later paper.) The Schrödinger equation for the motion in the z-direction is

$$\frac{\mathrm{d}^2\psi(z)}{\mathrm{d}z^2} + [\varepsilon - b^2(z - z_0)^2 - v\Theta(|z| - \tfrac{1}{2})]\psi(z) = 0. \tag{1}$$

The dimensionless variables in equation (1) are

$$\varepsilon = 2m^* a^2[E - \hbar^2 k_x^2/2m^*]/\hbar^2 \tag{2a}$$

$$v = V 2m^* a^2/\hbar^2 \tag{2b}$$

$$b = a^2 e B_\parallel/\hbar = a^2/R^2 \tag{2c}$$

$$z_0 = \hbar k_y/eB_\parallel a \tag{2d}$$

where E is the energy eigenvalue, k_x, k_y are the wavenumbers of electron propagation parallel to the potential walls, and m^* is the effective mass (which is different within the QW and in the barriers). An approximate solution of equation (1) can be obtained for comparatively low magnetic fields and strong barrier potentials. Then the effect

of the magnetic field on the electrons in the barrier is small compared to that of the barrier potential, and in the range $|z| > \frac{1}{2}$ equation (1) can be approximated by

$$\frac{d^2\psi(z)}{dz^2} + [\varepsilon - v]\psi(z) = 0. \tag{3}$$

This equation has the solution

$$\psi(z) = A_1 e^{\gamma z} + A_2 e^{-\gamma z} \qquad \gamma = \sqrt{v - \varepsilon}. \tag{4}$$

Normalization requires that $A_2 = 0$ in the left barrier, $A_1 = 0$ in the right barrier. Within the QW, for $|z| < \frac{1}{2}$, the solutions of equation (1) are expanded in a power series [1]:

$$\psi(z) = \sum_{n=0}^{\infty} \varphi_n z^n. \tag{5}$$

The boundary conditions for the solution of equation (1) are given by the continuity of the probability current density through the interfaces. They are satisfied if the total wavefunction and its first derivative are continuous. In the effective mass approximation the Bloch part of the wavefunction is taken into account in the effective mass and $\psi(z)$ represents the envelope function only. Bastard [6] argues that in this case the envelope function and its first derivative divided by the effective mass have to be continuous. In this paper we do not take into account the difference in the effective masses. (Johnson and MacKinnon [4] have shown how to handle effective-mass-differences via energy and effective mass-dependent barrier potentials.) The boundary conditions are thus the usual ones of matching the wavefunctions and their derivatives in $z = \pm\frac{1}{2}$. With the wavefunctions (4) and (5) the matching conditions result in the following set of equations for the expansion coefficients φ_n:

$$\sum_{n=0}^{\infty} \left(\frac{1}{2}\right)^{2n} \left(1 + \frac{4n}{\gamma}\right) \varphi_{2n} = 0 \tag{6a}$$

$$\sum_{n=0}^{\infty} \left(\frac{1}{2}\right)^{2n+1} \left(1 + \frac{4n+2}{\gamma}\right) \varphi_{2n+1} = 0. \tag{6b}$$

These equations have the same structure as the corresponding equations (2.7*b*) and (2.7*c*) of [1]. The effect of the finite barrier height can thus be incorporated into the treatment of [1] by changing the coefficients $A_{-2,2r} = (\frac{1}{2})^{2r}$ and $A_{-1,2l+1} = (\frac{1}{2})^{2l+1}$ to

$$A_{-2,2r} = \left(\frac{1}{2}\right)^{2r} \left(1 + \frac{4r}{\gamma}\right) \tag{7a}$$

$$A_{-1,2l+1} = \left(\frac{1}{2}\right)^{2l+1} \left(1 + \frac{4l+2}{\gamma}\right). \tag{7b}$$

We insert these coefficients into equation (2.9) of [1] for the determinant and expand the additional factors of $1/\gamma$ and $1/\gamma^2$ into an infinite power series of ε. The determinant of the coefficients is expanded as in [1]. Since the only difference is in the

boundary conditions the calculation of the minors is the same as for the infinite barrier potential. The resulting energy eigenvalue equation then has the same form as in the case of the infinite barrier height:

$$D = \sum_{f=0}^{\infty}\sum_{k=0}^{\infty}\sum_{g=0}^{\leqslant k/2} D_{f,g,k}(v)(-\varepsilon + b^2 z_0^2)^f b^{2k} z_0^{2g} = 0. \tag{8}$$

The only difference from equations (2.8) and (2.15*a*) of [1] is that the coefficients $D_{f,g,k}(v)$ are now functions of the barrier height v:

$$\begin{aligned} D_{f,g,k}(v) = {} & D^{\infty}_{f,g,k}(1 + 2(2f + 4k - 2g + 1)v^{-1/2}) + 4D''_{f,g,k}v^{-1} \\ & + \sum_{f'=0}^{f-1}(-1)^{f-f'}\left[D^{\infty}_{f',g,k}(2f' + 4k - 2g + 1)\frac{v^{f'-f-1/2}}{2^{2f-2f'-2}}\binom{2f - 2f' - 1}{f - f' - 1}\right. \\ & \left. + 4D''_{f',g,k}v^{f'-f-1}\right]. \end{aligned} \tag{9}$$

$D^{\infty}_{f,g,k}$ is the expansion coefficient for infinite barrier height given by equation (2.15*b*) of [1] and $D''_{f,g,k}$ is

$$\begin{aligned} D''_{f,g,k} = {} & 2^{-2f-4k+4g-1}\sum_{f'=0}^{f}\sum_{g'=0}^{2g}\sum_{h'=0}^{k-2g}(-1)^{g'}[2f' + 3g' + 4h'] \\ & \times {}_{-2}V_w(f', g', h')[2(f - f') + 3(2g - g') + 4(k - 2g - h') + 1] \\ & \times {}_{-1}V_w(f - f', 2g - g', k - 2g - h'). \end{aligned} \tag{10}$$

The coefficient ${}_uV_w$ is defined by equation (2.13) of [1]. The energy spectrum

$$E_n(k_x, k_y) = \frac{\hbar^2}{2m^*a^2}\varepsilon_n(v, b, k_y a) + \frac{\hbar^2}{2m^*}k_x^2 \tag{11}$$

results from the power series representation of ε:

$$\varepsilon = \varepsilon_n(v, b, \kappa_y) = \sum_{r=0}^{\infty}\sum_{t=0}^{r} G_{n;r+t,t}(v)b^{2r}\kappa_y^{2t} \tag{12a}$$

$$\kappa_y = k_y a$$

$$G_{n;r,t} = \begin{cases} 1 + G'_{n;r,t} & r = t = 1 \\ G'_{n;r,t} & \text{otherwise.} \end{cases} \tag{12b}$$

The $G'_{n;r,t}$ are determined via the recurrence relations (equations (13) correct some typographical errors in equations (2.17) of [1])

$$G'_{n;r,t} = \frac{-1}{N_s}\left[D_{0,t,r} + \sum_{l=1}^{\infty}(-1)^l\left(D_{l,0,0}M_{n;l,r,t} + \sum_{q=0}^{r-1}\sum_{m=0}^{t} D_{l,t-m,r-q}N_{n;l,q,m}\right)\right] \tag{13a}$$

$$M_{n;l,q,m} = \frac{1}{q(n\pi)^2} \sum_{k=1}^{q-1} \sum_{i=0}^{m} (kl - q + k) G'_{n;k,i} N_{n;l,q-k,m-i} \tag{13b}$$

$$N_{n;l,q,m} = M_{n;l,q,m} + l G'_{n;q,m} (n\pi)^{2(l-1)} \tag{13c}$$

$$N_s = \sum_{l=1}^{\infty} (-1)^l D_{l,0,0} l (G'_{n;0,0})^{l-1} = \cos\left(\sqrt{G'_{n;0,0}(v)}\right) \left(\frac{1}{4G'_{n;0,0}(v)} - \frac{1}{4\gamma^2} + \frac{1}{2\gamma^3}\right)$$
$$- \frac{\sin\left(\sqrt{G'_{n;0,0}(v)}\right)}{\sqrt{G'_{n;0,0}(v)}} \left(\frac{1}{4G'_{n;0,0}(v)} + \frac{1}{2\gamma} + \frac{1}{4\gamma^2} + \frac{G'_{n;0,0}(v)}{2\gamma^4}\right). \tag{13d}$$

The initial value $G'_{n;0,0}(v)$ is the energy in the absence of a magnetic field and results from the 'particle-in-a-box' eigenvalue equation

$$\tan \frac{\sqrt{G'_{n;0,0}(v)}}{2} = \begin{cases} \dfrac{\gamma}{\sqrt{G'_{n;0,0}(v)}} & n \text{ odd} \\ -\dfrac{\sqrt{G'_{n;0,0}(v)}}{\gamma} & n \text{ even.} \end{cases} \tag{14}$$

The energy spectra obtained from solving equations (11)–(14), e.g. on a PC, are discussed later in conjunction with the spectra obtained by exact numerical integration of equation (1).

The eigenfunctions of the QW states are obtained by inserting the energy eigenvalues into the parabolic cylinder functions which solve the Schrödinger equation (1). With the confluent hypergeometric functions $M(\alpha, \beta, \gamma)$ and the definitions

$$c := (-\varepsilon + b^2 z_0^2)/2b \qquad x := \sqrt{2b}(z - z_0) \qquad y := b\psi \tag{15}$$

the parabolic cylinder functions are

$$y_1(c,x) = e^{-x^2/4} M\left(\frac{c}{2} + \frac{1}{4}, \frac{1}{2}, \frac{x^2}{2}\right)$$
$$= e^{-x^2/4} \left[1 + \left(c + \frac{1}{2}\right)\frac{x^2}{2!} + \left(c + \frac{1}{2}\right)\left(c + \frac{5}{2}\right)\frac{x^4}{4!} + \ldots\right] \tag{16a}$$

$$y_2(c,x) = e^{-x^2/4} M\left(\frac{c}{2} + \frac{3}{4}, \frac{3}{2}, \frac{x^2}{2}\right)$$
$$= e^{-x^2/4} \left[x + \left(c + \frac{3}{2}\right)\frac{x^3}{3!} + \left(c + \frac{3}{2}\right)\left(c + \frac{7}{2}\right)\frac{x^5}{5!} + \ldots\right]. \tag{16b}$$

The coefficients of the appropriate linear combination of these functions and the coefficients A_1 and A_2 of the wavefunction in the barrier are determined by the boundary conditions and the normalization condition. These eigenfunctions are valid for $\varepsilon < v$. Their graphical representations agree very well with the wavefunctions obtained by exact numerical integration in section 3, cf, e.g., the lowest two and four density distributions in figures 3(*a*) and 3(*b*), respectively.

3. Numerical computation of the energy eigenvalues and eigenfunctions

In order to calculate the full energy spectrum without the restrictions and approximations necessary for the analytical calculations of section 2 we choose an appropriate matrix representation of the (dimensionless) Hamiltonian of the Schrödinger equation (1)

$$h = -\frac{d^2}{dz^2} + b^2(z - z_0)^2 + v\Theta(|z| - \tfrac{1}{2}). \tag{17}$$

A convenient set of basis functions is given by the (sine and cosine) eigenfunctions of a box with infinite potential walls in $za = \pm L_z$ where $L_z \gg a/2$. For sufficiently large L_z the eigenfunctions of equation (1) which decrease exponentially for $|z| \to \infty$ can be built up from this basis. With this basis the matrix representation of the Hamiltonian (17) contains the Fourier transforms of the harmonic oscillator and QW potentials. The Hamiltonian is diagonalized with the help of the Lanczos method [7]. The resulting energy eigenvalues and spectra are plotted in figures 1 and 2.

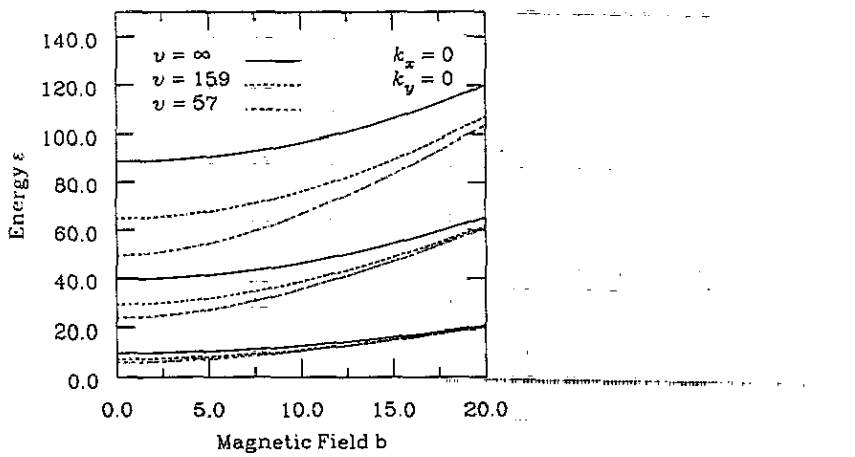

Figure 1. The lowest three energy levels, $\varepsilon = E2m^*a^2/\hbar$, of three QWs with different (normalized) barrier heights $v = V2m^*a^2/\hbar^2$ as functions of the (dimensionless) magnetic field $b = B_{||}ea^2/\hbar$. $m^* = 0.0665m_0$ is the effective mass of GaAs.

Figure 1 shows that in shallow QWs the increase in energy with increasing B field is stronger than in deep QWs. This is due to the fact that the tightening of the harmonic oscillator potential with increasing field reduces the spatial extension of the wavefunctions more in shallow than in deep QWs. (Note that ε, v and b scale with a^2, so that for a given a a smaller v means a shallower QW. $v = 159$ and $v = 57$ correspond to 20 nm and 12 nm wide QWs formed by GaAs between $Al_{0.3}Ga_{0.7}As$ at a conduction band offset of 60%, i.e. $V = 227$ meV.)

The energies calculated analytically from equations (11)–(14) of section 2 result in a plot very similar to that in figure 1. Quantitative agreement between the analytical and numerical results is excellent in the low field range. Deviations are largest for large b values, where the error of neglecting the magnetic field in the barriers is most severe. However, even then the deviations are somewhat small for all states within the QW, for which the analytical method has been developed: At $b = 20$ they are

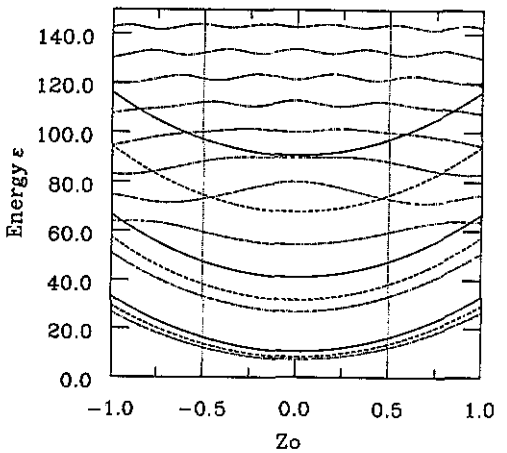

Figure 2. Energy spectra $\varepsilon(z_0)$, $z_0 = \hbar k_y/eB_{||}a$, of three different QWs for $b = 5$, $k_x = 0$. Full curves, $v = \infty$; broken curves, $v = 159$; chain curves, $v = 57$.

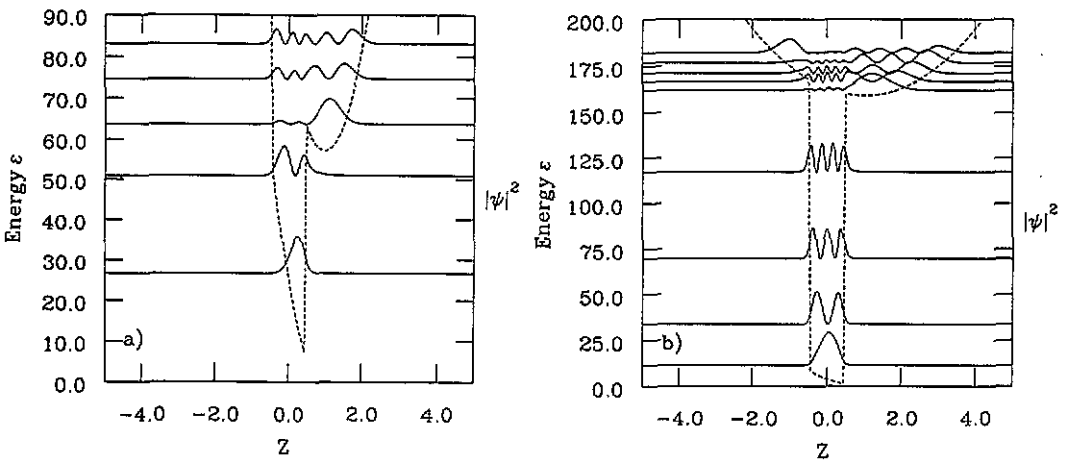

Figure 3. Spatial dependence of the effective potential v_{eff} (broken curve) and the electron density distribution $|\psi|^2$ plotted at the corresponding energy levels with $z_0 = 1$ for (a) $v = 57$, $b = 5$ and (b) $v = 159$, $b = 2$.

undetectable for the ground state energies, in the second subband the error is 1.2% for $v = 159$ and 7.7% for $v = 57$, and in the third subband for the QW with $v = 159$ the deviation is 5.6%. (Note that $v = 57$ and $b = 20$ corresponds to a magnetic field of 91 T.) For states outside the QW like the one of the uppermost chain line in figure 1 the analytical method breaks down and one has to rely on the numerical solutions alone.

For the bound states $\varepsilon < v$ the analytically calculated energy spectra agree with the numerical results shown in figure 2 within the drawing accuracy. As is to be expected from the spatial extent of the wavefunctions, the energies of shallow QWs are below the ones of deep QWs. For $v = 57$ the third and higher chain curves represent energies above v which no longer increase monotonically with z_0 (as do the ones below v). This is due to the fact that the width of the effective potential v_{eff} formed by the superposition of the square well and the harmonic oscillator potential with the minimum in z_0 may also increase with z_0 in this energy range. The flattening out of the

third subband for $v = 57$ indicates a localized barrier state [3] as can be seen explicitly in the charge density distribution of figure 3(a). A corresponding state appears in the fifth level of figure 3(b). These states are bound in the shallow depressions of v_{eff}. There is also a second type of barrier localization brought about by interferences; this is shown, e.g., in figure 3(b) by the density distribution of the ninth level for $z < 0$.

4. Conclusions

QWs in parallel magnetic fields represent systems whose energy spectra, well established by analytical and numerical calculations, can be tuned magnetically. This may make them useful magneto-optical devices. Experimental detection of the localized barrier states may be possible by resonant Raman scattering: Electrons pumped optically into the subband system recombine with the holes in the valence band via the emission of a phonon and a photon. The resulting frequency shift in photoluminescence depends upon the phonon energy which is different in GaAs and $Al_xGa_{1-x}As$, and the intensities of the two different Stokes peaks indicate the probability density distributions between the well and barrier of the involved electrons [8].

Acknowledgment

This work was supported in part by the Deutsche Forschungsgemeinschaft. All the numerical calculations of section 3 were done on the VAX 8810 and VAX 6000-420 of the Rechenzentrum der Universität Würzburg.

References

[1] Huckestein B and Kümmel R 1987 *Z. Phys.* B **66** 475
[2] Huckestein B and Kümmel R 1988 *Phys. Rev.* B **38** 8215
[3] Johnson E, MacKinnon A and Goebel C J 1987 *J. Phys. C: Solid State Phys.* **20** L521
[4] Johnson E and MacKinnon A 1988 *J. Phys. C: Solid State Phys.* **21** 3091
[5] Maan J C 1984 *Springer Series in Solid State Science* vol 53 (Berlin: Springer) p 183
[6] Bastard G 1981 *Phys. Rev.* B **24** 5693
[7] Haydock R, Heine V and Kelly M J 1972 *J. Phys. C: Solid State Phys.* **5** 2845
[8] Lier K 1991 *Diplomarbeit* Universität Würzburg unpublished
Schüller C 1991 private communication